From: COASTAL OCEANOGRAPHY
Edited by Herman Gade, Anton Edwards, and Harald Svendsen
(Plenum Publishing Corporation, 1983)

CONSIDERATIONS OF COASTALLY FORCED FLOW IN A BRANCHED FJORD

John M. Klinck, Benoit Cushman-Roisin* and James J. O'Brien*

Texas A&M University
Department of Oceanography
College Station, TX 77843 U.S.A.
*Florida State University, Tallahassee, Florida 32306, U.S.A.

ABSTRACT

Two techniques are combined to consider the dynamics of a narrow, stratified fjord system with two channels.

The first technique removes the barotropic mode from a two layer model but retains the influence of bottom topography. The second technique allows development of a numerical model of two narrow, connected channels. The resulting branched fjord model is forced by coastal wind stress through the mechanism of Ekman flux. The major question addressed with this model is, what determines the exchange between the two channels in a time dependent situation.

Various simulations are performed with different widths, depths, and lengths for the channels and locations for the junction. From the simulations three main conclusions are obtained:

1) The presence of a side channel increases greatly the variability of the forced flow in the main channel.

2) Geometric constrictions (sills and narrows) have only local effect on the flow if the flow remains subcritical.

3) The relative lengths of the two channels have the strongest effect on the variability of the resulting flow.

INTRODUCTION

The Ryfylkefjord system, comprising the Boknafjord, Sandsfjord, Hylsfjord, Saudafjord and others (Fig. 1), is a geometrically complicated interconnection of deep narrow channels and is typical of many fjord systems. Such a dynamical system can be analyzed with a three dimensional numerical model, but such models are expensive to develop and to run. This paper presents a model that approximates such geometric complexity in a way that is inexpensive enough for many situations to be examined.

A basic method for connecting channels depends on the use of a spatially-staggered numerical grid, with transport and thickness variables at alternating grid points. All connections between two channels are chosen to occur at thickness grid points. This procedure was first suggested by Dr. D. P. Wang (see Elliot, 1976) and was used in a model of Chesapeake Bay (Wang and Elliot, 1978).

Another procedure has been proposed by Narayanan (1979) in a study of the barotropic tidal response of the Douglas Channel along the coast of British Columbia. The linear wave propagation problem is solved for each tidal frequency, by following a non-staggered path of integration and introducing a certain number (say N) of arbitrary transport and depth values where necessary (junctions and open boundaries). The integration is performed N times with different values assigned to those constants. The solution is then sought as a linear combination, such that all flow constraints (also N in number) are met. In a second stage, the linear tidal response is used to initialize a non-linear model, using an explicit scheme. The basic limitations of Narayanan's procedure are two-fold: (i), for each frequency, the algorithm sweeps the system N+1 times and solves an N by N full linear system; (ii) the method of unknown constants cannot be generalized to non-linear models, while the initialization by a linear solution may fail in the study of baroclinic motions (particle velocity closer to wave speed).

The present model is based on Wang's method, to keep the number of passes over the system to a minimum of one Gaussian elimination per time step (or per frequency, if a modal decomposition were applied), and to open the way to direct and accurate extension to non-linear dynamics.

We chose to investigate narrow, deep silled fjords with a linear, two-layer, nonrotating model. The model is externally forced by coastal wind stress through Ekman flux. We ignore diffusively driven flow, such as that due to freshwater addition from rivers, and the effects of wind stress in the fjord itself. The simplified dynamics allow us to focus on the interaction of flow in several channels. Diffusion and local forcing can be considered as the understanding of the multibranched fjord system increases.

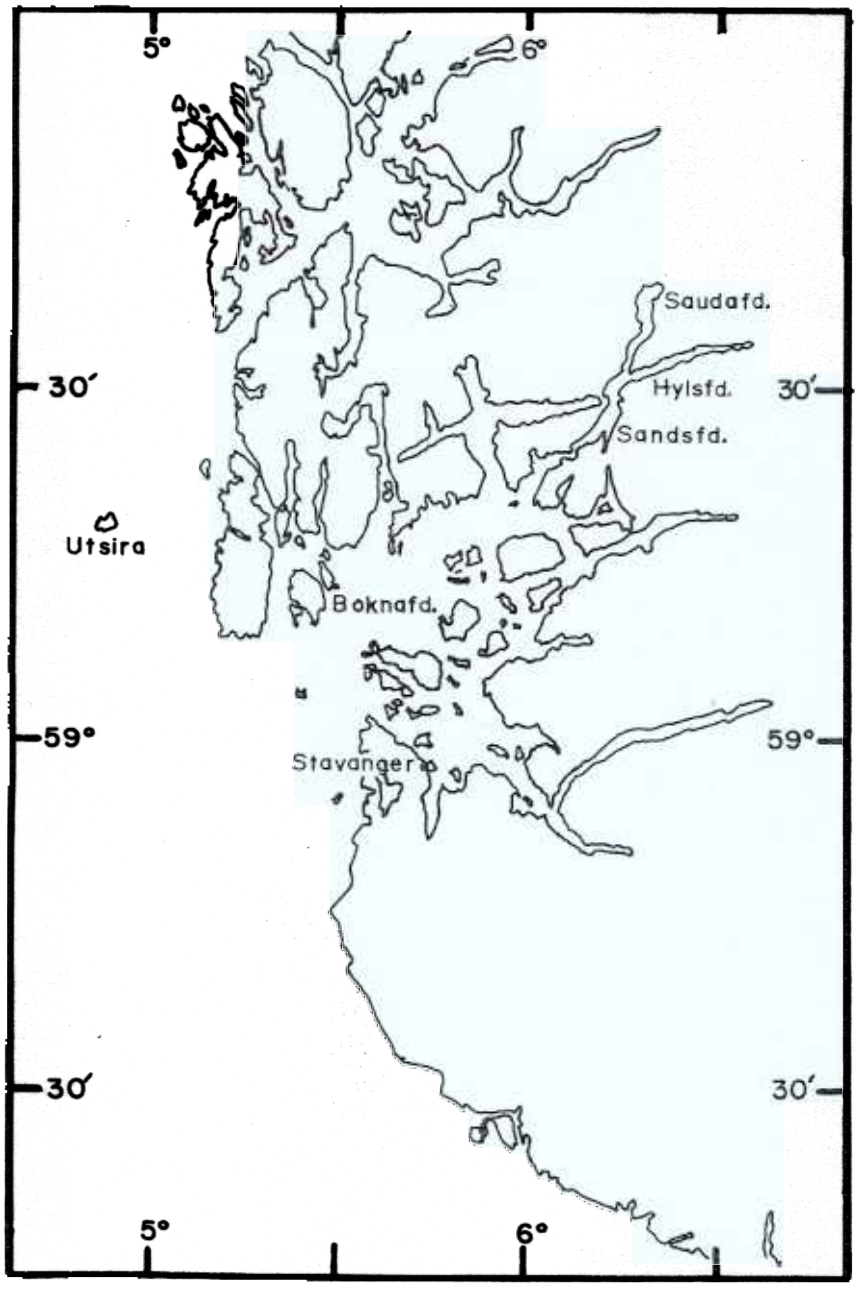

Fig. 1. Map of the Ryfylkefjords on the western coast of Norway

The following questions are considered in this study. How do long gravity waves behave in a system with two channels? What controls the exchanges between the two channels? How do sills and narrows influence the exchange between the two channels?

The following section considers the dynamical equations and the procedure for eliminating the barotropic mode while retaining the effects of bottom topography. Section III presents the numerical technique for connecting two narrow channels. The details of the numerical model are also discussed. Several simulations are discussed in Section VI. The effect of geometry and topography are presented. Section V summarizes the paper and lists conclusions.

EQUATIONS

a) Two-layer Model

The dynamics of a narrow, stratified fjord are investigated with a linear, two-layer, vertically and laterally integrated model. The governing equations are

$$U_{1t} = -gH_1W(h_1 + h_2 + D)_x + K\,U_{1xx} + W\tau^x$$

$$U_{2t} = -gH_2W(h_1 + h_2 + D)_x + K\,U_{2xx} + g\frac{\Delta\rho}{\rho}\,H_2Wh_{1x}$$

$$h_{1t} = -\frac{1}{W}U_{1x}$$

$$h_{2t} = -\frac{1}{W}U_{2x}$$

The geometry of the model is indicated in Fig. 2 and the variables are given in Table I. Note that U_i is the total mass transport (cm^3/sec) of a given layer.

The local surface stress is included in (1) but its influence is not considered here. Also included in each layer is a horizontal friction term. The coefficient is chosen so that frictional effects are not dynamically important and only provide a small amount of smoothing.

If the bottom is horizontal, these equations can be decoupled into two independent modes as outlined by Veronis and Stommel (1956). Each of the modes satisfies a one-layer, long gravity wave equation but the wave speed is different for each of the modes. To be more explicit about the modal separations, a linear combination of the variables is defined as

$$U = U_1 + \lambda U_2 \quad \text{and} \quad h = h_1 + \lambda h_2$$

Table I - Notation

A:	area of junction region
c:	local baroclinic wave speed
D:	depth anomaly
g:	acceleration of gravity
	undisturbed thickness for layer i
H:	total volume of junction region
	thickness of layer i (main channel)
$\hat{h}_i$:	thickness of layer i (side channel)
K:	horizontal diffusion coefficient
$\hat{L}$:	number of grid points in the main channel
t:	time
U_i:	volume transport for layer i (main channel)
$\hat{V}_i$:	volume transport for layer i (side channel)
W:	width of main channel
$\hat{W}$:	width of side channel
x:	position along main channel (positive toward head)
y:	positive along side channel (zero at junction, positive towards head)
$\alpha\pm$:	squared speed of barotropic (+) and baroclinic modes
	density of layer i $\rho_1<\rho_2 = \rho$)
	density difference between layers $(\rho_2 - \rho_1)$
	structure coefficient for $\pm$ mode
η:	average elevation of junction region
μ:	a function of order unity
τ^y:	surface wind stress

and the modal variables are required to satisfy an equation of the form

$$U_t = -\alpha W h_x + K U_{xx} - \alpha\lambda W D_x + W\tau^x$$

$$h_t = -\frac{1}{W} U_x$$

The parameters α and λ must satisfy algebraic consistency relations, which reduce to a quadratic equation for α (or λ). The character of these parameters is easily shown in the limit of small $\Delta\rho/\rho$, which is $O(10^{-3})$ in most oceanic situations.

The approximate parameters, expanding in $\Delta\rho/\rho$, are

$$\lambda_+ = 1 \qquad \alpha_+ = g(H_1 + H_2)$$

and

$$\lambda_- = -\frac{H_1}{H_2} \qquad \alpha_- = g\frac{\Delta\rho}{\rho}\frac{H_1 H_2}{H_1+H_2} \tag{4}$$

The parameters denoted by the plus subscript correspond to the barotropic mode while the negative subscripts denote the baroclinic mode. Each alpha is the square of the celerity for the surface and internal gravity waves.

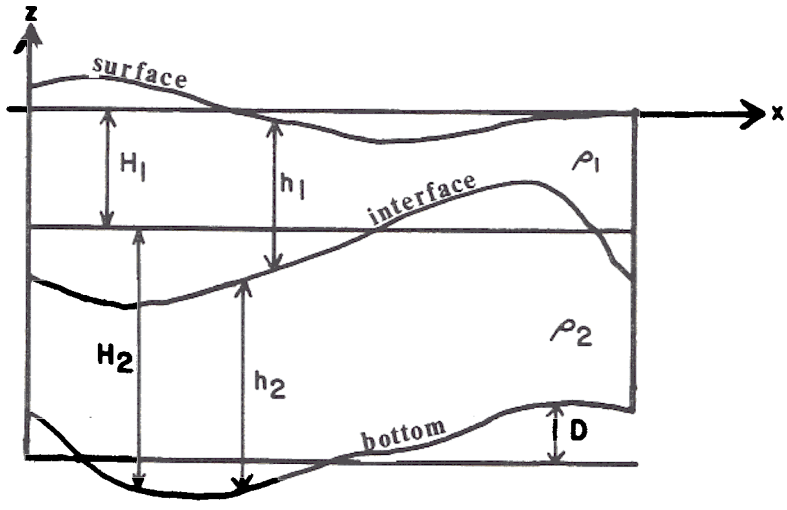

Fig. 2. Model geometry and variables.

If topography effects are present (H_2 function of x), the above method of modal decoupling fails because of the interaction between the fast and slow motions: Passing a topography feature, a barotropic wave generates a baroclinic component and vice versa (Proudman, 1953). And,the more abrupt is the topography, the greater is that interaction. Therefore, only approximate methods can be developed to decouple the barotropic and baroclinic modes in the presence of bottom topography, and their accuracy depends on the strength of the coupling. To consider the barotropic mode in isolation, one simply sets H_2, h_2, U_2 to zero and lets H_1 be the total undisturbed depth. This is equivalent to neglecting $\Delta\rho$ in Equation (1). The accuracy is thus only $\Delta\rho/\rho$.

If the baroclinic mode is to be studied in isolation, the elimination of the barotropic mode is not so simple. The usual procedure involves an infinitely deep, passive, lower layer (the reduced-gravity model). This procedure also eliminates the effect of bottom topography. Its accuracy is H_1/H_2.

b) Baroclinic Model

In order to study the baroclinic mode in isolation while retaining the influence of bottom topography, a new procedure has been developed. It uses the fact that the baroclinic mode has almost no vertically integrated transport to eliminate the barotropic mode from the two-layer model. That is, from (4), $U_2 = -U_1$ to lowest order in $\Delta\rho/\rho$.

First, define h to be the displacement of the free surface from its reference position or $h = h_1 - H_1 + h_2 - H_2$. The two-layer equations (1) are rewritten (with K, $\tau^x = 0$) as

$$U_{1t} = -gH_1 W h_x$$

$$U_{2t} = -gH_2(x) W h_x + \frac{\Delta\rho}{\rho} gH_2(x) W h_{1x}$$

$$h_{1t} = - U_{1x} \frac{1}{W} \quad h_{2t} = - U_{2x} \frac{1}{W}$$

since $D_x = -H_{2x}$.

Assume that

$$U_2 = -\left[1 + \frac{\Delta\rho}{\rho}\mu(x,t)\right]$$

where μ is a function (to be determined) of order unity. The system of equations (5) can be reduced to the single equation:

$$(\mu U_1)tt = g(H_1 + H_2)W\frac{\partial}{\partial x}\left[\frac{1}{W}(\mu U_{1x}\right] + gH_2W\frac{\partial}{\partial x}(\frac{1}{W}U_{1x}). \qquad 7$$

The time derivative term is of order $\Delta\rho/\rho$ compared to the other two terms in this equation. Indeed, it will be shown a posteriori that the baroclinic mode satisfies a wave equation which allows replacement of two time derivatives with the phase speed times two space derivatives. Since the baroclinic phase speed is approximately $\alpha^{-1/2}$, replace $\partial^2/\partial t^2$ with $\alpha - \partial^2/\partial x^2$, where $\alpha -$ is defined in (4). The first term is clearly of order $\Delta\rho/\rho$ compared to the other two terms.

If the function μ varies slowly in x or

$$\mu_x << U_x \qquad (8)$$

then the solution for μ is

$$\mu(x) = -H_2(x)/(H_1 + H_2) \qquad (9)$$

Condition (8) requires that the bottom topography vary slowly over a wavelength of the internal wave.

Now that $\mu(x)$ is known, the equations for the baroclinic mode

$$\begin{aligned} U_{1t} &= -c^2(x)Wh_{1x} \\ h_{1t} &= -\frac{1}{W}U_{1x} \end{aligned} \qquad (10)$$

where $c^2(x) = \frac{\Delta\rho}{\rho}g\frac{H_1H_2}{H_1+H_2}\left|1 + \frac{\Delta\rho}{\rho}\frac{H_1H_2}{H_1+H_2}\right|$, which is the square of the "local" baroclinic phase speed. Once U_1 and h_1 are calculated, U_2 is obtained from (6), and h_2 from an identical relationship.

The approximations have eliminated the coupling between the baroclinic and barotropic modes. Such coupling occurs through nonlinear interaction (hydraulic processes) or through creation of internal waves by barotropic flow over sharp bottom topography. It is therefore concluded that the coupling is weak and negligible (on the order of $\Delta\rho/\rho)^2$) as long as velocities are much smaller than the phase speeds and the topography smooth over one wavelength.

c) External Forcing

The effects of an along shore coastal wind on flow in a fjord are investigated with a coastal upwelling model and a fjord model which join at the coastline (Klinck, et al., 1981). The results of this study are paraphrased here: a more complete discussion is contained in the reference cited.

The first conclusion from the coupled model is that the coastal wind stress forces flow in the fjord through Ekman transport. The wind pumps water either in or out the upper layer at the ocean mouth of the fjord. The changes at the mouth induced by the forcing travel to the rest of the fjord as long gravity waves.

The second conclusion is that the barotropic disturbance created by changes in the wind is very quickly in balance (in a few hours for a 50 km long fjord) and thus the dominant response in the fjord is baroclinic. It is for this reason that we choose to focus on the baroclinic mode and its interaction with width and depth variations in the fjord.

The results of this previous study show that a coastal boundary condition can be imposed on the baroclinic wavefield. However, specifying the baroclinic transport at the ocean boundary is improper because it does not allow waves to leave the fjord and generates spurious reflections of waves. Fortunately, these reflected waves do not affect the interaction of the two channels. Therefore, for the present work, the model is forced by an imposed baroclinic flow at the ocean boundary, simulating the baroclinic flow.

DETAILS OF NUMERICAL MODEL

a) Branching Technique

The procedure for connecting two narrow channels uses the modal equations (3). As such, the technique can be used for any multilayer model for which linear, nonrotating dynamics are appropriate.

The basic method for connecting a side channel to a main channel depends on the use of a spatially staggered numerical grid with transport and thickness variables at alternating grid points. The connection between the two channels occurs at a thickness grid point (see Fig. 3). That is, the two channels share a common grid point (called the junction). This procedure was first suggested by Dr. D. P. Wang (see Elliot, 1976) and was used in a model of Chesapeake Bay (Wang and Elliot, 1978).

The junction region is defined by the dashed lines in Fig. 3. The conditions at the junction are

1) continuity of thickness and,

2) conservation of mass.

The first condition is satisfied automatically since the two channels share a common thickness point.

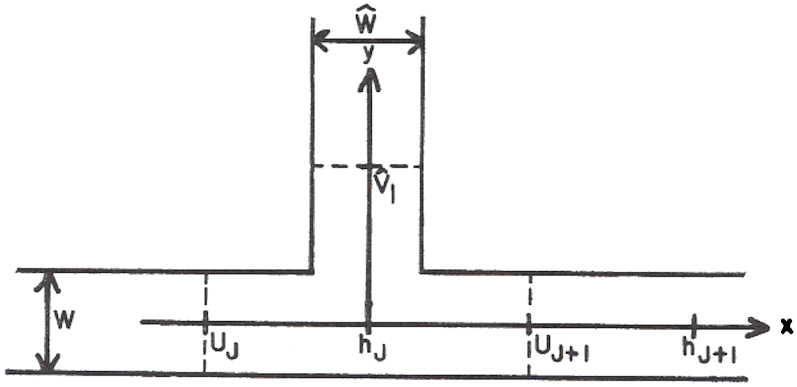

Fig. 3. Geometry of the junction region and staggered grid.

The second condition is obtained by integrating the continuity equation over the junction region,

$$H_t = U_j - U_{j+1} - \hat{V}_1 \qquad (11)$$

For notational clarity, the main channel is along the x axis while the side channel is along the y axis. Variables with a caret refer to the side channel. H refers to the total volume of the junction region. This expression cannot be used directly in (3), but must be modified somewhat. Let A be the surface area of the junction region then the average interface elevation is $\eta = H/A$. Therefore, the continuity condition becomes

$$\eta_t = (U_j - U_{j+1} - \hat{V}_1)/A$$

This development simply yields a modified continuity condition at the single grid point at the junction.

The branching condition is strictly kinematic, so inertia (dynamic) effects at the junction are ignored. This choice requires that the flow in the junction be slow enough that such inertia effects are negligible. The precise condition is $u^2 \ll c^2$ where c is the gravity wave speed for the mode under consideration. This condition is obtained by scaling the full momentum equation. The condition that $u^2 \ll c^2$ is also required for the flow in the channel

to be subcritical - a choice which is already made by the use of linear dynamics.

Since inertia effects are unimportant in the junction region, the angle between the two channels is not important. This assumption may not be strictly valid for some fjord situations where the junction is near a narrow (or shallow) region of the fjord.

The mathematical problem is now specified and can be solved by a number of numerical techniques.

b) Numerical Model

The simplest numerical procedure is an explicit time integration of the equation in the two channels. Although this method is the simplest, it can prove quite costly because the time step is limited by the CFL stability condition,

$$\Delta t < \frac{\Delta x}{\sqrt{2}\, C_{max}}$$

where C_{max} is the maximum wave speed allowed by the dynamics. In this case, the maximum speed is the barotropic wave speed. The CFL condition can be quite restrictive for deep fjords.

The use of the baroclinic equation allows a large enough time step for the calculation to be practical. This fact provided the impetus to derive the baroclinic equations in the first place.

Since part of this work will compare the two-layer model with the baroclinic model, another approach is taken. The equations are integrated with a semi-implicit technique which is unconditionally stable. This technique uses implicit time differences on the terms in the equations which give rise to the fastest waves. Phase errors are introduced for the barotropic waves but as the waves do not participate actively in the overall circulation of the fjord, these errors are not important (see Grotjahn and O'Brien, 1976, for a discussion of the phase errors). The unconditional stability of this integration procedure allows the choice of any time step consistent with a reasonable truncation error.

However, this ability to chose a large time step has a price a set of linear equations must be solved at each time step. This linear system must be amenable to a direct and fast solution algorithm for the semi-implicit method to be computationally more efficient than an explicit method.

For a one channel model, semi-implicit integration gives rise to a linear system with a tridiagonal matrix which can be solved with an "up-down" algorithm that is fast and direct. When the

semi-implicit method is used on the equations for the branched system, the coefficient matrix of the resulting linear system is "almost" tridiagonal. The "up-down" algorithm can be modified to account for the off-tridiagonal terms yielding a direct solution scheme. The appendix presents the details of the linear system and of the solution procedure.

Both the two-layer model and the baroclinic model were constructed using the semi-implicit integration scheme. Several test calculations were made to compare the two models. For a variety of depth and width variations, the two models give identical results. The remainder of this paper considers simulations from the baroclinic model alone.

SIMULATION AND DYNAMICS

The effects of width and depth changes in a fjord are now considered with the baroclinic, branched model that is forced by coastal Ekman flux. Particular emphasis is placed on the factors which determine how the flow divides at the junction, and how the two channels interact in a time-dependent situation.

The parameters for the simulation (Table II) are chosen to correspond to fjords like the Ryfylkefjords. Data for these fjords are provided by Svendsen (1981). The wind forcing is chosen to simulate the reversals of coastal wind which are observed offshore of the Ryfylkefjords (Svendsen, 1981). To simplify interpretation of the model simulations, the wind is taken to be a sinusoid with a 5 day period. The magnitude of the wind is 2 dynes/cm^2 which gives an average velocity at the fjord mouth of 10 cm/sec.

a) Case I

The first case presented has a main channel length of 60 km and a side channel 40 km long. The junction is 20 km from the mouth of the fjord. This geometry yields identical distances from the junction to the end wall in both channels. Since gravity waves travel at the same speed in each channel, the waves will split at

Table II

$H = 20$ m	$U(x=0) = 10. \times H_1 \times W \times \sin(2\pi t/60\text{hr})$
$H = 480$ m	$\Delta\rho/\rho = .002$
$W = \hat{W} = 1$ km	$\Delta x = 2$ km
$K_x = K_y = 10^5$ cm^2/s	$\Delta t = 1$ h

the junction and return in phase after a reflection from the end wall.

Fig. 4 is a phase plot of the pycnocline anomaly for the situation just described. It is evident that the pycnocline disturbance in the branch is the same as that in the main channel between the junction and the end wall. This fact shows that the junction region does not introduce any phase shifts or affect the flow in an unrealistic manner. Also included on the figure is one characteristic to show that the semi-implicit integration scheme does not affect the phase of the gravity waves in the simulation.

To address the question of exchange between the two channels, velocity is shown as a function of time (Fig. 5) for the first velocity grid point in the side branch and for the first velocity point toward the head of the fjord from the junction. The speeds into each channel have the same magnitude and the same variation. This fact is expected since both channels have the same cross sectional area, thus splitting the flow equally between the two channels. The velocity does not show a sinusoidal disturbance, from the sinusoidal forcing, because waves reflect from the end wall and mix with the waves produced by the direct forcing. There is also

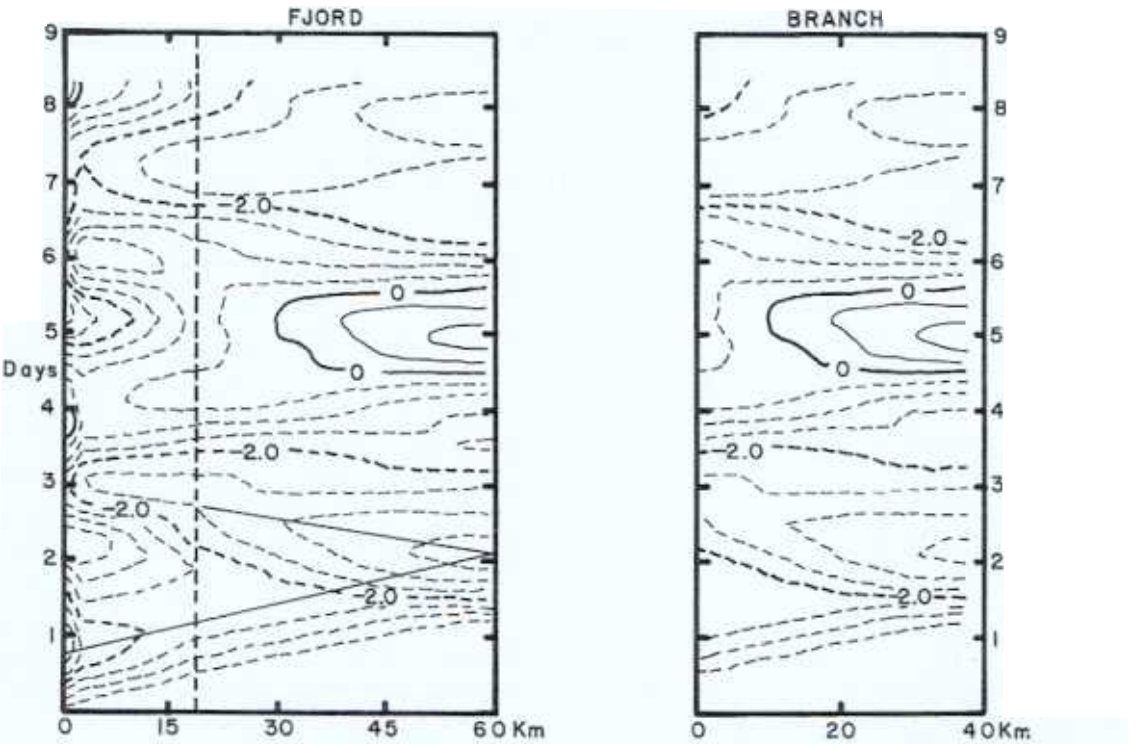

Fig. 4. Pycnocline anomaly for Case I. Ocean forcing has a 5 day period. Solid line denotes a characteristic. Contour interval is .5 m. The junction is denoted by the vertical dashed line.

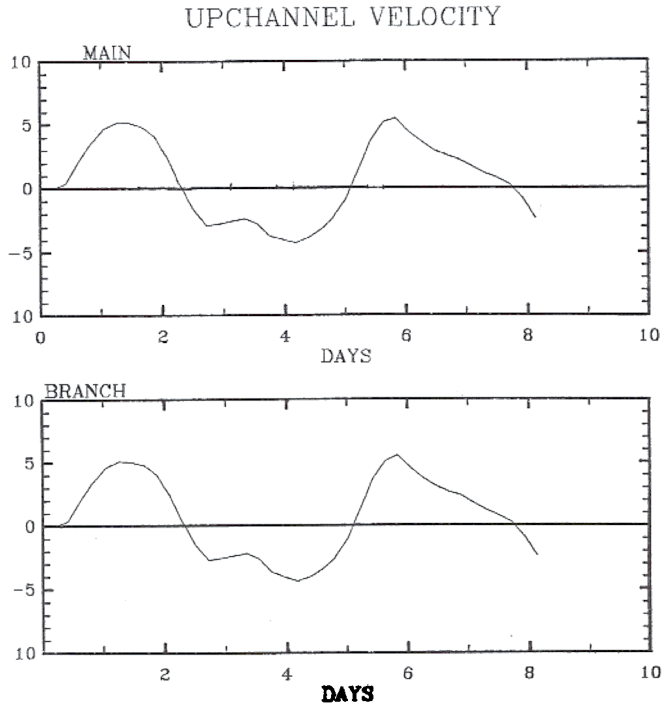

5. Case I. Velocity variation from the first grid point from junction toward the head of the main and side channels. Units are cm/sec.

some spurious reflection from the ocean mouth of the fjord due to the choice of boundary condition there.

b) Case II

The second case is a slight modification of the first case. The main and side channels are 40 km long and the junction is 10 km from the ocean boundary. Now the two channels have different lengths from the junction to the end walls. The pycnocline anomaly (Fig. 6) is not the same in the two channels, but is greater in the longer branch. To see the variation in the flow more easily,

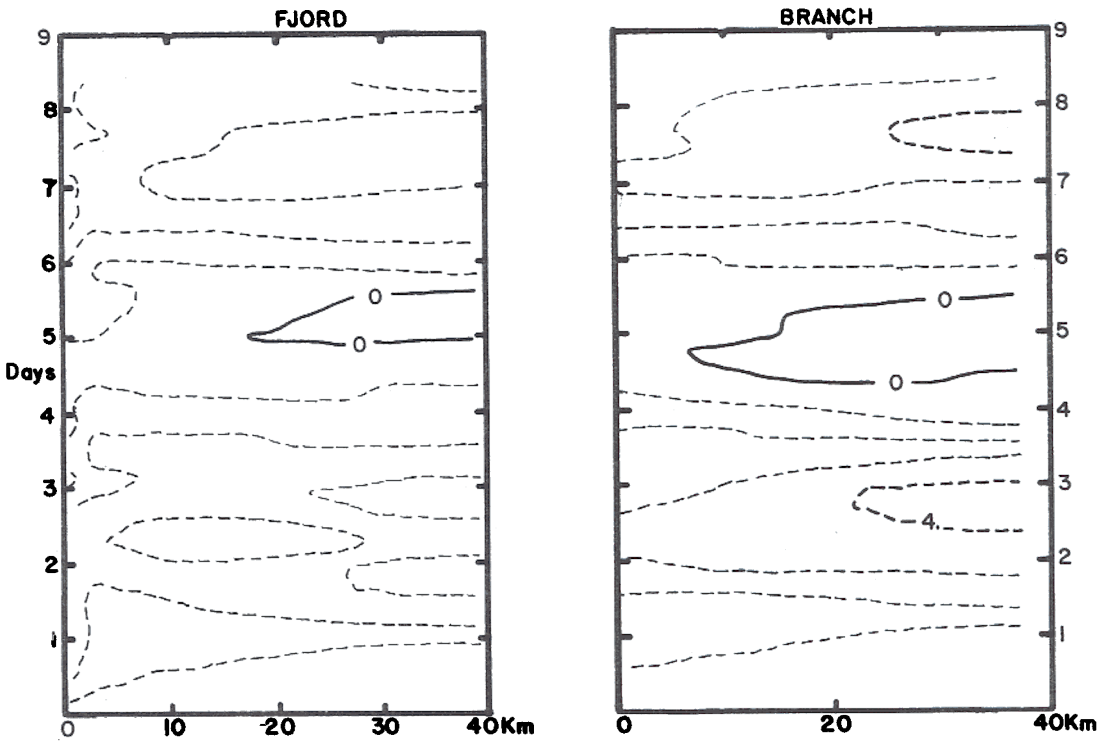

Fig. 6. Pycnocline anomaly for Case II. Contour interval is 1 m

consider the time plot of the velocity at the entrance to each branch (Fig. 7). Note that after the first two days, the velocity is quite different in the two channels. This difference is due to the phase of the waves when they return to the junction. This phase difference can be seen easily through ray tracing arguments (not presented here). From Fig. 7 it appears that there has been a net increase (over the first eight days) in the volume of water in the main channel downstream of the junction while the side channel shows no increase in volume. These differences in transport are due strictly to length differences of the two channels since both channels have the same width and depth.

c) Case III

Case III considers the effect of channel width on the branched system. The side channel has a constant width of .5 km while the main channel is 1 km wide. The geometry of Case I is retained so the two channels are the same length from the junction to the end wall.

The pycnocline anomaly looks the same as Fig. 4, so only the velocity time history is shown (Fig. 8). The velocity shows the

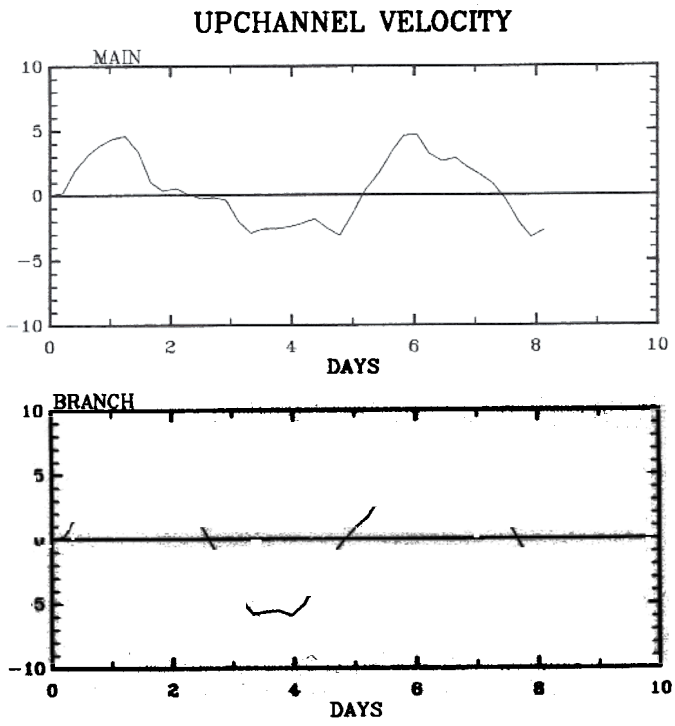

Fig. 7. Case II velocity variation. Units are cm/sec.

same structure as Fig. 5 but the amplitude is larger in both branches. The increase in speed over case I (15%) is proportional to the decrease in total volume of the fjord system due to the narrower side channel.

This simulation shows that the transport divides at the junction in proportion to the cross sectional area of the two "downstream" channels, where "downstream" depends on the direction towards which the wave is moving. This division of the transport by cross sectional area produces the same velocity for each of the downstream channels even though the transport into each channel may be quite different.

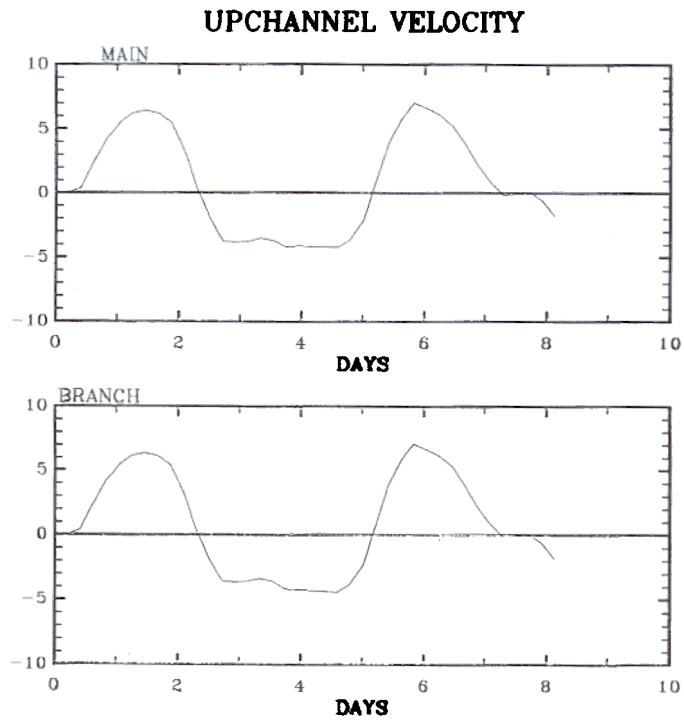

Fig. 8. Case III velocity variation. Units are cm/sec.

d) Sills and Narrows

Several simulations were calculated to consider the effect of sills and narrows on the exchange between two channels. These simulations had sills that were 200 m high or narrows to .5 km in one branch just inside the junction. None of these simulations are shown here because these constricting effects had only a local effect on the flow: the flow was greater in proportion to the decrease in cross sectional area. The presence of a sill narrows in one channel had no effect on the exchange at the junction. Therefore, for the dynamics included in this model, only the local geometry of the junction region and the relative lengths of the two channels have any influence on the exchange between the two channels in a branched fjord.

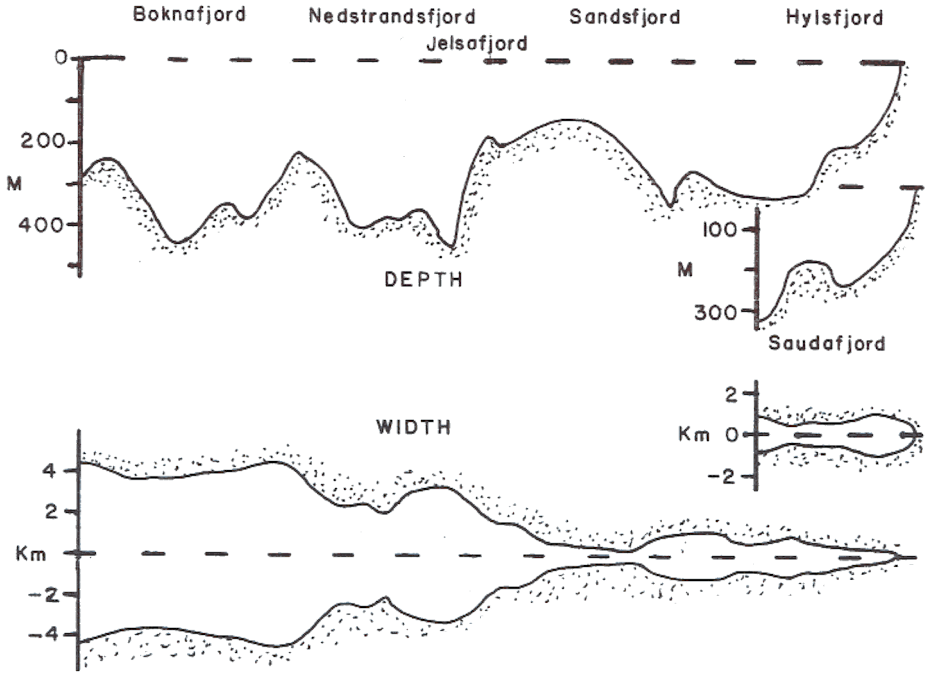

Fig. 9. Width and depth for Sandsfjord - Saudafjord system.

This conclusion assumes that there are no hydraulic effects in either channel. If a sill or narrows causes the flow to speed up sufficiently to be supercritical, then this region becomes a control section and must influence flow both up and downstream of that region.

For deep-silled fjords which do not have hydraulic controls, the baroclinic model should simulate the dynamics adequately, and the geometry of a given branched fjord determines the exchange between the two channels.

e) Sandsfjord System

The ultimate aim of this research is to analyze an actual fjord having two channels. Towards that end, one simulation is included which considers a part of the Ryfylkefjord system. Because of the 2 km resolution of the model, the width and depth must be smoothed somewhat to match the model resolution. Fig. 9 displays the smoothed width and depth profiles for the main channel (Boknafjord to Hylsfjord) and the side channel (Saudafjord).

One simulation with this complicated geometry is performed with forcing by a five-day period Ekman flux. The pycnocline anomaly is presented in Fig. 10. The most notable feature of this simulation is that the largest flows, indicated by the largest pycnocline anomaly, appear at constrictions in the channel. It is difficult to

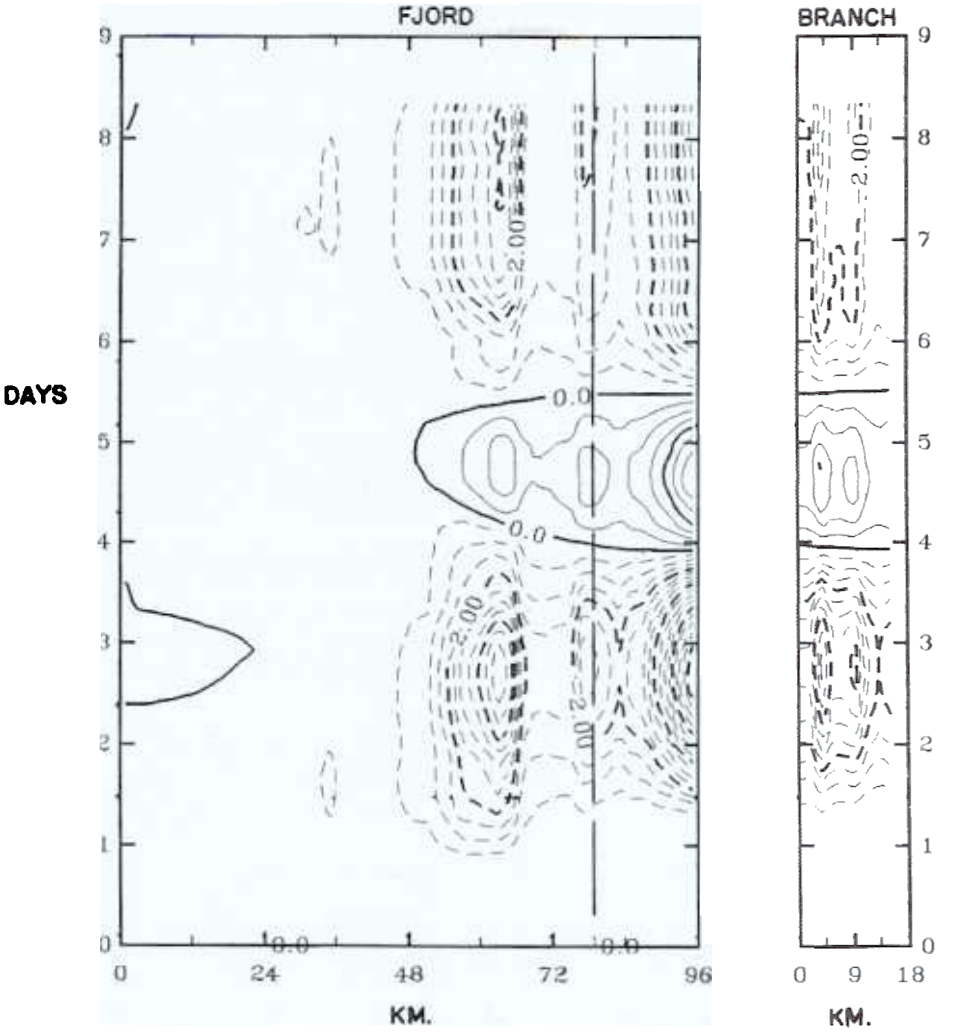

Fig. 10. Pycnocline anomaly for the Sandsfjord - Saudafjord geometry. Contour interval is .5 m.

detect much of the disturbance between the constrictions.

The exchange between the two channels is considered in Fig. 11. The velocities are not very different over the 20 day span of this simulation, but the length of Hylsfjord and Saudafjord differ by only 2 km (Fig. 9), and their topographies are quite close. Therefore, the waves return to the junction at about the same time. Notice that even though the forcing has a 5 day period, the presence of a side channel allows extra freedom to the waves in the system and the disturbance at a given point does not reflect the forcing period at all. The geometry of the Sandfjord system does not provide a

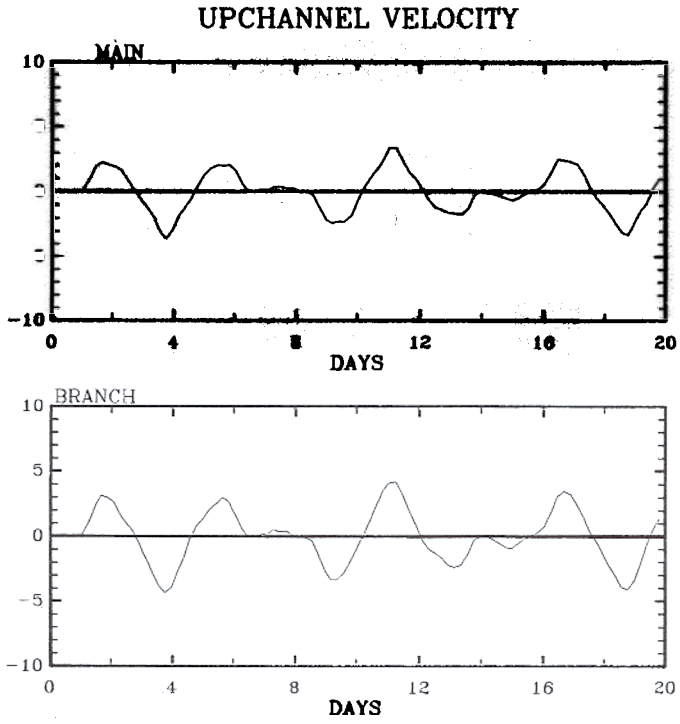

Fig. 11. Velocity variation for Sandsfjord - Saudafjord simulation. Units are cm/sec.

sensitive test of the exchange processes because the two channels are so close in length and topography. A better place to consider exchanges might be the Jøsenfjord branch off the main channel.

Since constrictions in a narrow channel amplify the flow so markedly, as illustrated by Fig. 10, one speculates that these regions would show the strongest response to coastal wind events. It may also be that for a strong coastal wind storm, the flow in some constriction may become critical and develop a hydraulic jump. As the storm slackens, such a jump would be released as an internal bore or solitary wave. It would be interesting to see if coastal storms produce such jumps or enhanced mixing in constriction far removed from the direct effect of the wind.

COASTALLY FORCED FLOW IN A BRANCHED FJORD

SUMMARY

Two techniques are combined to consider dynamics of a narrow, stratified fjord system with two channels.

The first technique removes the barotropic mode from a two-layer model but retains the influence of bottom topography. Earlier baroclinic models removed the barotropic mode by having a passive, infinitely deep lower layer. Such an assumption is not appropriate for fjords.

The second technique allows a numerical model to be constructed which connects two narrow channels. Only kinematic conditions of conservation of mass and continuity of the interface are specified. Therefore, there are no inertia effects at the junction and the angle between the two channels is not important.

The branched-fjord model is forced by coastal wind stress through the mechanism of Ekman flux. The major question addressed here is what determines the relative exchange of the two channels in under time dependent circumstances.

Various simulations are calculated with different widths, depths and lengths for the two channels and different choices for the location of the junction of the two channels. From the simulations, three main conclusions are obtained:

1) The presence of a side channel increases greatly the variability of the forced flow in a narrow channel.

2) Geometric constriction (sills and narrows) have only a local effect on the flow if the flow remains subcritical.

3) The relative lengths of the two channels have the strongest effect on the variability of the resulting flow.

ACKNOWLEDGMENTS

This work was supported by the National Science Foundation grant OCE-7925351. The authors are indebted to Dr. David Farmer suggesting additional references.

REFERENCES

Elliot, A.J., 1976, A numerical model of the internal circulation in a branching tidal estuary, Chesapeake Bay Institute, The Johns Hopkins University, Special Report 54, Ref. 76-7.

Grotjahn, R., O'Brien, J.J., 1976, Some Inaccuracies in Finite Differencing Hyperbolic Equations, Mon. Wea. Rev., 104:180.

Klinck, J.M., O'Brien, J.J., Svendsen, H., 1981, A simple model of Fjord and Coastal Circulation Interaction, J. Phys. Oceanogr., 11:1612.

Narayanan, S., 1979, Kitimat physical oceanography study 1977-1978. Tidal circulation model, Dobrocky SEATECH Ltd. Report, Victoria, British Columbia.

Proudman, J., 1953: Dynamical Oceanography, Methuen & Co. Ltd., London, pp. 349-351.

Svendsen, H., 1981: A Study of the Circulation and Exchange Processes in the Ryfylke fjords, Vol. I and II, University of Bergen, Report 55.

Veronis, G., Stommel, H., 1956, The Action of Variable Wind Stresses on a Stratified Ocean, J. Mar. Res., 15:43.

Wang, D.-P., Elliot, A.J., 1978, Non-Tidal Variability in the Chesapeake Bay and Potomac River: Evidence for non-local forcing, J. Phys. Oceanogr., 8:225.

APPENDIX

The linear algebraic system of equations to be solved at each step of the semi-implicit integration is denoted

$$\mathbf{M}\,\bar{u} = \bar{f} \qquad \text{(A1)}$$

Where M is the coefficient matrix, $\bar{u}$ is a vector of the transport at the new time and $\bar{f}$ is the forcing obtained in terms of variables at the old time steps. The vector $\bar{u}$, is obtained by concatenating the main channel variables and the side variables, $\bar{u} = (U_1, U_2, \ldots, U_L, \hat{V}_1, \ldots, \hat{V}_L)$. The almost tridiagonal matrix is shown in Fig. Ala where the asterisks indicate non-zero matrix elements and the solid circles indicate the off tridiagonal elements that result from the branching condition.

The "up-down" algorithm is modified in the following way to form an "insweep-outsweep" procedure. The insweep step involves Gaussian elimination of the matrix elements below the diagonal from the ocean to the junction. A similar procedure eliminates the elements above the diagonal starting at the end of each channel and moving towards the junction. Fig. Alb shows the form of the matrix at the end of the insweep part of the solution.

The matrix elements denoted by asterisks correspond to U_J, U_J +1 and $\hat{V}_1$, which are the three transport variables defining the junction region (Fig. 3). These matrix elements compose an independent, fully dense 3 x 3 linear system to be solved for the three transport variables, analogous to the coefficient matrix

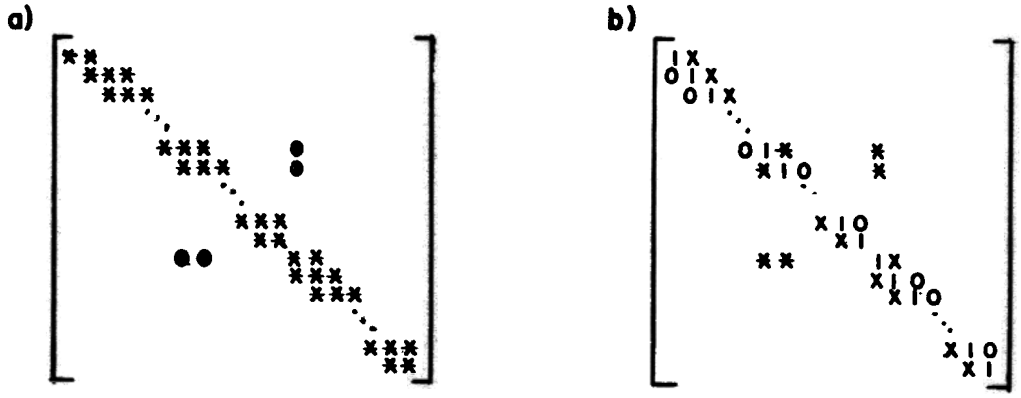

Fig. A1. Coefficient matrix for the branched model. a) asterisks denote non-zero matrix elements. Solid circles denote the "off tridiagonal" elements due to branching. b) After insweep. X's denote changed elements. Asterisks define a 3 x 3 matrix for the three velocity point defining the junction.

obtained by Narayanan (1979). This 3 x 3 can be solved directly by Gaussian elimination.

Once these three values are known, the "outsweep" part of the procedure finds the values of the adjacent transport variables until the complete solution is known.

This modified tridiagonal solution scheme requires the computation of an ordinary "up-down" solution plus that for the solution of a 3 x 3 linear system. This procedure gives a fast and direct solution to the linear system and justifies the use of a semi-implicit integration scheme over an explicit calculation (for the two-layer model).